Fatigue behaviour assessment of C45 steel by means of energy-based methods

Fatigue behaviour assessment of C45 steel by means of energy-based methods

R De Finis[1], D Palumbo[1], A Pirinu[2], A Saponaro[2], F W Panella[2], R Nobile[2], U Galietti[1]

[1]Politecnico di Bari – Dipartimento di Meccanica, Matematica e Management, Via Orabona 5, Bari (BA)
[2] Università del Salento-Dipartimento di Ingegneria dell'Innovazione, Lecce - Monteroni - Lecce (LE)

rosa.definis@poliba.it

Abstract. Methods and techniques presented in literature for studying the fatigue behaviour of materials involve expensive, long lasting experimental campaigns and often a data analysis providing any information about damage localisation and occurrence. To avoid a time-consuming mechanical characterisation and to provide more information about where and when damage is occurring, the full-field experimental techniques such as infrared thermography allows the assessment of parameters that are related to the energy conversion to heat. In this work, the relationship between these thermal parameters (thermal methods) sentinels of the energy dissipated per cycle and the energy absorbed in every cycle is presented for the C45 steel undergoing stepwise loading fatigue tests.

1. Introduction

Thermography a full-field non-destructive experimental technique is nowadays widely used for the analysis and study of reversible and irreversible energy heat sources that appear in the material when a cyclic load is imposed [1–16].

By exploiting the appropriate and relatively simple setup, and a specific loading procedure (stepwise loading) [11] an accelerated fatigue test campaigns (just 5 specimens being tested) can be carried out allowing researchers to obtain an estimation of the fatigue endurance limit in a few hours of testing and analysis [1–14]. Moreover, by carrying out specific data processing algorithms of the thermographic data, the localization of the damage and the assessment of the time instant at which damage occurs are provided. So that, by using experimental techniques for fatigue characterization, more information about the material state are available together with the damage monitoring. Conventional method for fatigue characterization, such as 'Staircase' method [1], require at least 15 specimens being tested and a total duration of the experimental campaign up to 2/3 months.

As shown in [1], there are many approaches adopted up to now and based on the detection of the thermal radiation. In particular they are aimed at studying parameters such as:

- the mean temperature increase of the specimens [4], [5], [9–14],
- the reversible or irreversible thermal heat sources [2], [3], [15], [16-18]
- the phase of the thermoelastic signal (TPA method) [6,9-10].

Luong [2] in his work, adopted an energetic approach that studied the the intrinsic dissipations of the material by measuring the surface temperature variations. In this work, Luong proposed a graphic method for assessing the fatigue limit. Morabito [4] and Risitano [5] proposed similar approaches for performing fatigue tests at gradually increasing load amplitudes up to the failure (stepwise loading procedure of the test). In fact, if the load stresses exceed the fatigue limit, the surface temperature of the specimen presents a trend defined by an initial increase and a subsequent plateau. Therefore, by considering only the values reached in the stable phase or the temperature increases (ΔT / ΔN) as a function of the number of cycles, the damage can be studied. These two procedures involves a linear regression analysis of the data to find the fatigue limit.

The 'local energy' approach, on the other hand, is based on the study of the terms of the diffusion equation to separate the intrinsic heat sources related to processes within the material, both reversible (thermoelastic sources) and irreversible (dissipative phenomena) [15-18]. However, this type of approach requires a considerable amount of information to be analyzed and well-structured algorithms to be implemented. Meneghetti [3] by performing an energy approach, considered the “specific energy loss” during the fatigue test due to the heat dissipated per unit of volume and per cycle (Q parameter). To assess the parameter a suitable procedure has to be implemented requiring to arrest instantaneously the fatigue test. Each one of these approach is based on the hypothesis that the material presents a temperature stabilization trough the cycles, otherwise, some others considerations are required to assess the best parameter.

Another approach is to evaluate thermoelastic heat sources. For example, Krapez [6] and Galietti [9] carry out the analysis of the thermal signal to obtain the harmonic components. In this way the study of the fatigue behavior is carried out by studying the variations of the phase shift and amplitude components obtained. The Thermoelastic Stress Analysis [19–22] is based on evaluating the surface stress level based on thermoelastic effect (small temperature variations induced by volume variations) when the material is experiencing a cyclic load in linear-elastic field [8-9]. In case of adiabatic conditions are present during the test for an isotropic and homogenous material, the surface stress invariant and the amplitude of the thermal signal at the mechanical frequency are proportional [22]. When damage occurs the stress/temperature relationship becomes non-linear, but the significant variation in thermoelastic signal can be a guideline to detect the onset of the damage [6,20]. The termoelastic phase shift is another tool to investigate the material behaviour as it is zero in case of linear elastic conditions and varies in presence of damage processes [23].

In the work of Enke [7], another component of the thermal signal is represented by the second amplitude harmonic that is in that approach related to double increase of plastic deformation during a loading cycle. This component seems to be related to the energy dissipated in the material as presented in [8].

The presented approaches allow the fatigue behavior assessment of metallic (regular shape [1] [9] [10] or notched [11] and complex shaped [8] [13]).

Despite the multiplicity of approaches in literature, in order to evaluate the fatigue behavior it is necessary to highlight that the thermal signal is influenced by noise sources which must be taken into account as they can compromise the analyses. The temperature parameter is influenced by several factors (i.e. environmental temperature), due to this issue as demonstrated in [23], a more specific analysis of the temperature components is required to be able to detect local phenomena and to make accurate estimations on material behaviour. The analysis of the components of the thermal signal is more promising in the fatigue behaviour investigation as it exploits parameters directly related to energy, volume variations, non-adiabatic conditions.

The approaches based on assessment of the energy absorbed by material during cyclic loading [24] are useful to draw considerations on material residual strength. In effect, the accumulation of fatigue damage is governed by the plastic deformation [25]. The area under the hysteresis loop is correlated to the damage accumulation and in turn is also related to the load amplitude. Such relationship is a rather important real and practical problem because this energy seems to be a convenient measure of the accumulated fatigue damage [26]. However, the energy absorbed per cycle by a material can be

evaluated by applying an extensometer in the gage length [10] or by using full-field techniques such as digital imaging correlation (DIC) [18]. The first technique is not common in practical problems on complex shaped components while the DIC requires the application of a speckle pattern on material surface that it is not always possible.

Several researchers, focused on the relation between the energy dissipated as heat and energy related to hysteresis loop [7-10]. It is clear that temperature variations are somehow an estimation of the total energy provided to the material but can be useful in those application where it is difficult to measure the energy involved in mechanical hysteresis.

The aim of the present work is to study the fatigue behaviour of C45 steel by using energy-based methods related to energy absorbed by the material and energy converted in heating, and to highlight the possible correlation between second amplitude harmonic temperature component and value of the area under the hysteresis loop.

2. Material and methods

The material tested in this work is the tempered steel C45 widely used in the mechanical sector for the construction of shafts, cranks, keys, pins, supports, rods, drive shafts.

In order to obtain static properties of the material tensile tests (5 tests) were performed by using a displacement rate of 1 mm / min that provided the following data in terms of ultimate tensile strength of about 732 MPa (dev.st 30.60 MPa) and a yield stress of 463 MPa (dev.st 60.91 MPa).

The tested "dog bone" specimens were designed according to ASTM E 466-96 [27], the cross section was 12x6 mm^2 and the gage length was 30 mm. Two experimental campaign were carried out at two stress ratios (R) 0.1 and -1. A total of 3 specimens were tested for each experimental campaign at fixed stress ratio.

A servo-hydraulic machine manufactured by MTS (model 370 with a capacity of 100 kN) was used to perform the fatigue tests. To obtain the temperature measurements it was used the FLIR SC 6540 thermal imaging camera with a 640x512 pixel cooled sensor and a thermal sensitivity less than 30 mK. In order to increase the emissivity of the monitored surfaces it was applied a matt black paint (emissivity 0.95).

The setup is described in figure 1.

The test procedure consists of a sequence of loading steps applied gradually (stepwise loading) according to table 1 [1] at the same frequency and R. The stress was applied with a frequency of 17 Hz (11 Hz for R=-1) and maintained for about 20,000 cycles of the loading machine [9]. The mechanical frequency was lower for the tests running at R=-1 due to avoid temperature variation higher than 150°C. At the end of the cycles of each step, the stress was increased, as shown in (Table 1), until the material failure. The test duration is roughly 150,000.00 cycles.

To describe the material behaviour the initial loading block are characterised by loads starting from a maximum stress of 20-30% of the ultimate tensile strength (UTS). This ensures to have a sufficient number of data points under the fatigue limit. The increment between a stage and another, in terms of stress amplitude ($\sigma_a=\Delta\sigma/2$), is variable: it ranges between 5-20 MPa and 20-40 MPa for respectively the points near the fatigue limit and far away from the fatigue limit both for the test at R=0.1 and R=-1. It results from a compromise to describe accurately the material behaviour (to have sufficient data) and to maintain the test duration competitive with respect to standard test methods.

During the test, thermographic acquisitions are performed at 175 Hz for 10 seconds (1775 frames acquired) and at 123 Hz for 10 seconds (1223 frames acquired) for the tests at R=-1. The thermal sequence of each loading step is acquired at a number of cycles that corresponded to the material temperature stabilisation: about 15,000 cycles for each loading block.

To acquire hysteresis loops in terms of force and strain data, a contact clip-on extensometer with a 25 mm gauge length was used. The frame rate used for acquiring mechanical data was 200 Hz in all the tests. The extensometer acquired continuously during the whole test duration.

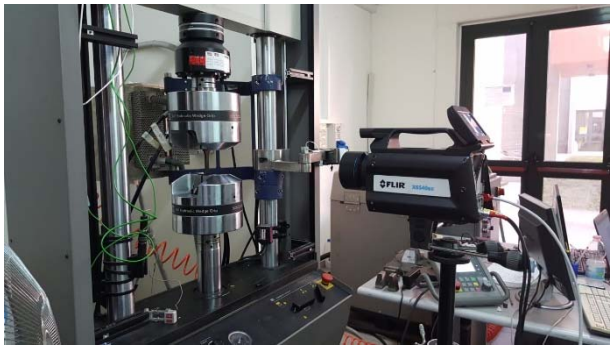

Figure 1. Equipment and layout: loading frame and infrared thermal camera.

Table 1. Assigned loading table to C45 steel at R=0.1 and R=-1.

σ_{med} (MPa)	σ_a (MPa)	σ_{med} (MPa)	σ_a (MPa)
123	101	0	185
145	119	0	200
167	137	0	230
189	155	0	245
206	168	0	260
211	173	0	275
217	177	0	290
222	182	0	305
228	186	0	320
233	191	0	340
244	200	0	360
272	222	0	380
299	245	0	420
327	267		
354	290		

3. Data Analysis

3.1. Thermal Signal Analysis

In a fatigue test where the loading stress is above the fatigue limit, the measured surface temperature exhibits a typical trend (figure 2). This trend is composed by three phases: a first stage of temperature increase occurring in the first cycles, a second stabilization stage before the last phase with an abrupt increase up to the material failure [5]. In order to perform correctly the analysis one has to refer to the temperature achieved in such a steady state condition (ΔT_{max}, figure 2) to extract proper parameters.

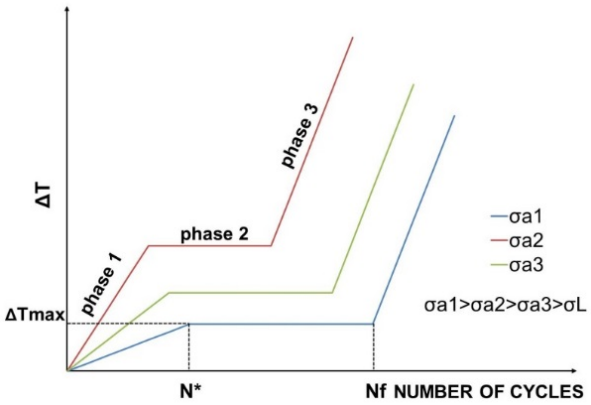

Figure 2. Theoretical temperature evolution for different loading levels [1].

Although in presence of a damage, the temperature (ΔT_{max}) tends to increase, it is necessary to consider all the thermal sources producing 'noise' blurring the signal that can affect the measurement [1]. Therefore, considering the generic pixel in the useful section of the specimen, the temperature can be characterized as follows:

$$T(x,y,t) = f[T_{amb}(t), T_d(x,y,t), T_{lm}(x,y,t)] \quad (1)$$

Where t is the generic time instant and the terms: T_d, T_{lm}, T_{amb} respectively indicate the temperature increase due to dissipative phenomena, the temperature increase due to the heat flow transferred to the specimen through the clamps of the servo-hydraulic machine and the one due to the effect of room temperature. As the only quantity linked to the damage processes is T_d, it is necessary, for the purposes of the analysis, to filter out the other two thermal sources.

Another way to approach the problem is to consider the components of the thermal signal that are quantities related to specific energetic aspects due to specific physical phenomena and can be used for more local qualitative and quantitative analysis [9-10],[23].

Based on a signal reconstruction algorithm performed by using a least square method, the thermal signal analysis provides the decomposition of the thermal signal T(t) in linear and non-linear components. The following model is used to assess thermal components and then to extract pixels by pixels maps representing the different parameters:

$$T(t) = T_0 + at + T_1 \sin(\omega t + \varphi) + T_2 \sin(2\omega t + \varphi_2) \quad (2)$$

where $T_0 + at$ is the linear part of the temperature signal, T_1 and φ are the amplitude and phase of the first component of the temperature signal that is related to the thermoelastic signal [18-20], T_2 and φ_2 are the amplitude of the thermal signal linked to the dissipative sources and the phase shift between the first and the second harmonic components [23].

The algorithm based on the model of equation (2) is implemented on the software Irta [28].

In the present study the analyses are focused on the following parameters: T_0, T_1,φ,T_2. Different algorithms have been developed for the data processing of each one and implemented in Matlab® routines. The whole processing procedures of thermal parameter are referred to the region of interest that is the gage length of the samples.

In figure 3 the four different processing procedures are presented.

The temperature variations related to the intercept of the linear part the model described by equation (2), T_0, is a parameter related to the mean temperature increase. It is influenced by the just said heat sources, hence the step of the processing involve:

- Elimination of the effect of environment (room temperature) by just subtracting the mean value of the temperature measured on a dummy specimen [23];

- Elimination of the conduction gradient from hottest loading grip [23] by supposing a linear temperature increase due to this effect from hottest to coldest grip;
- To reduce the noise in the map a spatial filter (median kernel) was applied on maps;
- From each map the 95^{th} percentile value was extracted as a parameter, in order to avoid outliers.
- The assessed parameter was $\Delta T_{0_{95prc}}$

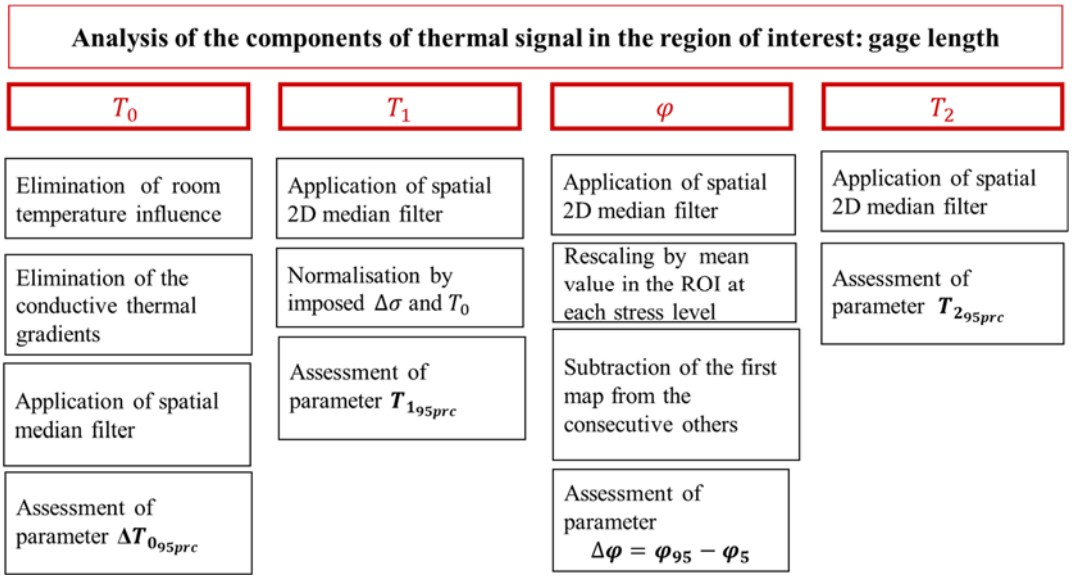

Figure 3. Procedure for the data processing of thermal parameters.

T_1 raw maps of the gage length of the samples were treated by using the following procedure:

- Application of spatial median filter, the same filter type adopted for the previous parameter;
- The signal, was after, normalised by the stress amplitude and the mean value in the gage length of T_0;
- From each map the 95^{th} percentile value was extracted as a parameter, in order to avoid outliers.
- The assessed parameter was $T_{1_{95prc}}/\Delta\sigma$ and also the parameter $T_{1_{95prc}}/T_0\,\Delta\sigma$;

  This latter was evaluated in order to eliminate both the effect of mean temperature and stress amplitude on thermoelastic signal.

Thermoelastic phase shift φ raw maps were treated by following the procedure:

- Application of spatial median filter, the same filter type adopted for previous parameters;
- Rescaling by the mean value of the data in the gage length to emphasize the minimum and maximum values;
- Subtraction the phase map of the first loading levels to the maps of the following levels to eliminate the noise of the loading level where damage is absent;
- From each resulting maps 95^{th} and 5^{th} percentiles were extracted and the difference $\Delta\varphi$ was evaluated as parameter for studying fatigue behaviour.

The processing of T_2 raw maps involved the following steps:

- Application of spatial median filter, the same filter type adopted for the previous parameter;
- Extraction from each map the 95^{th} percentile value as a parameter for studying the fatigue behaviour, the choice of percentiles instead of the maximum is to avoid data outliers.
- The assessed parameter to study damage was $T_{2_{95prc}}$.

3.2. Hysteresis loop measurement

To obtain the area under the hysteresis loop per cycle, the data obtained by the extensometer have been processed. The processing procedure is the same for both experimental data at R=0.1 and R=-1.

The procedure, figure 4, was implemented in a Matlab® routine and involved the following stages:

- the assessment of the strain-stress data couples. As it is well-known the extensometer provides the strain-load data series, so that the stress can be evaluated be considering the sample cross section area previously measured;
- the considered hysteresis loops refer to the material stabilisation: 5 hysteresis loops have been took into account at about 15,000.00 cycles of each loading block;
- for each curve, a discrete approximated numerical integration was performed via trapezoidal method to assess the area under the hysteresis loop;
- for each stress level, the mean value through 5 previously evaluated areas under hysteresis loop was considered as the energy-based parameter $\Delta \boldsymbol{W}$.

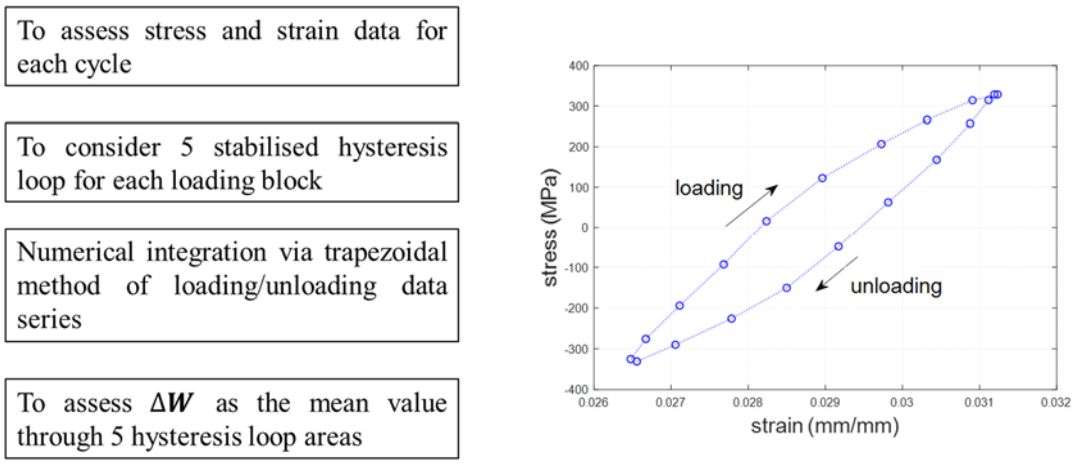

Figure 4. Procedure for the data processing of strain-stress data.

In the following section the results in terms of the parameter obtained by each energy-based method are presented and discussed together with the discussion of possible relationship between parameters and the final qualitative study of the maps from thermal parameters.

4. Results and discussion

In the present section the thermal parameter maps and the curves resulting from the analysis of thermal and mechanical signals are presented and discussed.

4.1. Qualitative analysis of the data: maps of thermal parameters

In the present section the maps of the parameters obtained by thermal processing adopted in section 3.1 are presented.

The maps in figure 5 represent respectively the parameter ΔT_0, T_1, $\Delta\varphi$,T_2 in the gage length of a tested sample (sample 2) at stress ratio of 0.1.

In the ΔT_0 maps of figure 5a signal increase is evident from a stress level (σ_a) higher than 180 MPa. A similar consideration on signal increase starting from 180 MPa can be drawn for both T_1 (figure 5b) and T_2 (figure 5d) while the signal maps of $\Delta\varphi$ exhibit a significant signal increase at σ_a=186 MPa where some localised regions experienced maximum and minimum signal increase (figure 5c). From the maps in figure 5 one can draw the considerations that ΔT_0 allows describing the overall damaging area while the amplitudes and phase provide local information related to different physical phenomena.

The figure 6 show the maps of thermal parameters of the tests at R=-1 for the sample P2. ΔT_0 maps of figure 6a a signal that is continuously increasing from initial stress level to the last, the temperature increase in correspondence of σ_a=310 MPa is such high that a separate scale value was adopted to represent this latter map. The maps in figure 6a show a signal increase in the middle of the gage length while T_1 maps (figure 6b) show a gradient from upper to lower part of the ROI affecting the thermoelastic temperature variations while the initial signal increase mostly interested lower part of the sample. This can be due the occurrence of heat sources from different sites running at the loading frequency just before the material failure. The phase data (figure 6c) are characterised by noisy phase maps until σ_a=275 MPa while higher signal from the left side of the gage length just before the failure is present due to the ongoing damage. The temperature variations related to intrinsic dissipations (figure 6d) present a significant signal increase only at σ_a=310 MPa and localised sites of higher signal spread in the gage length.

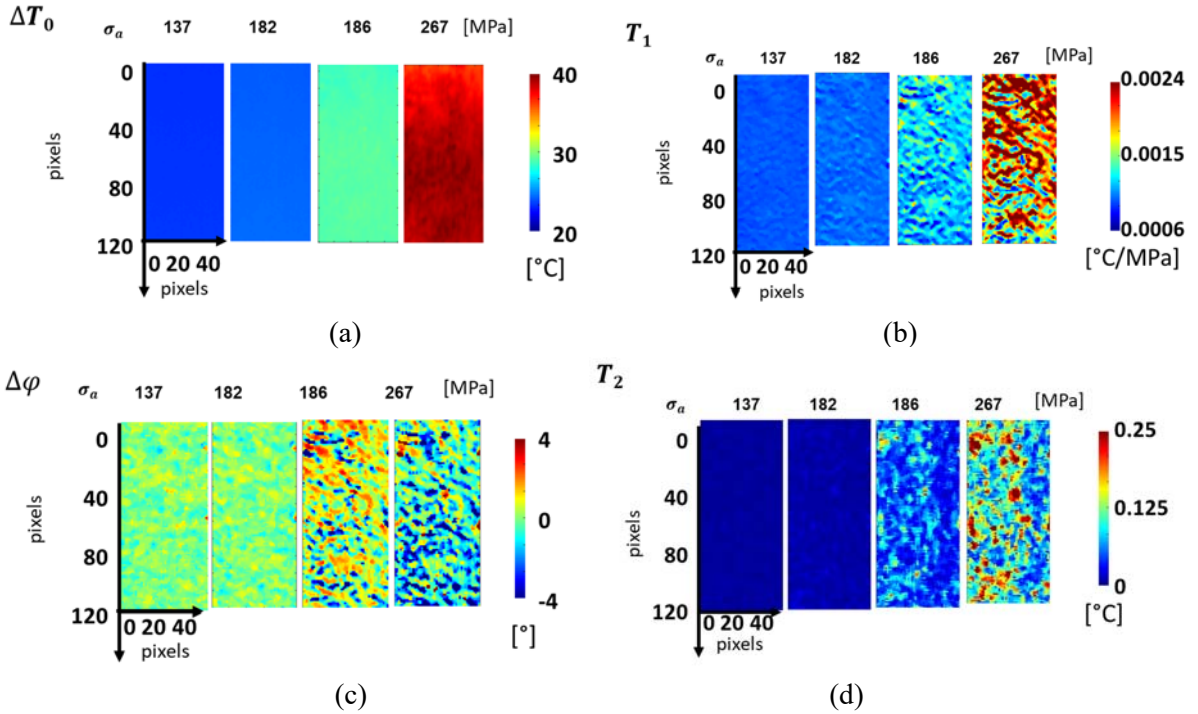

Figure 5. Maps resulting from the analysis of energy-based methods related to thermal parameters at R=0.1, sample P2.

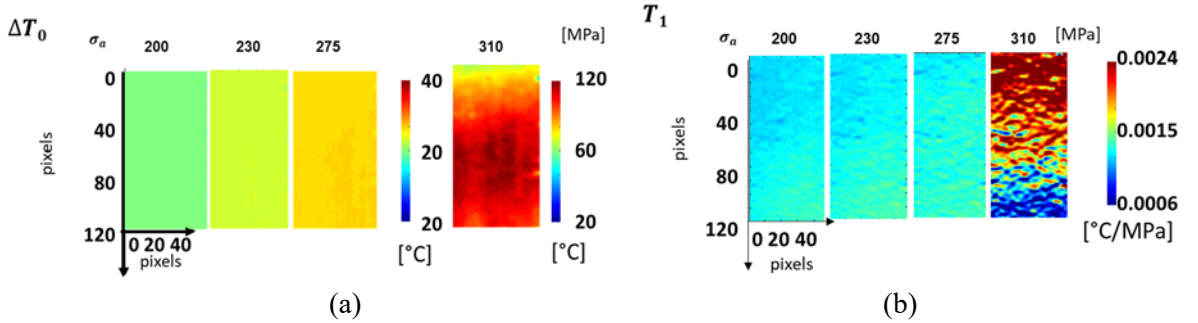

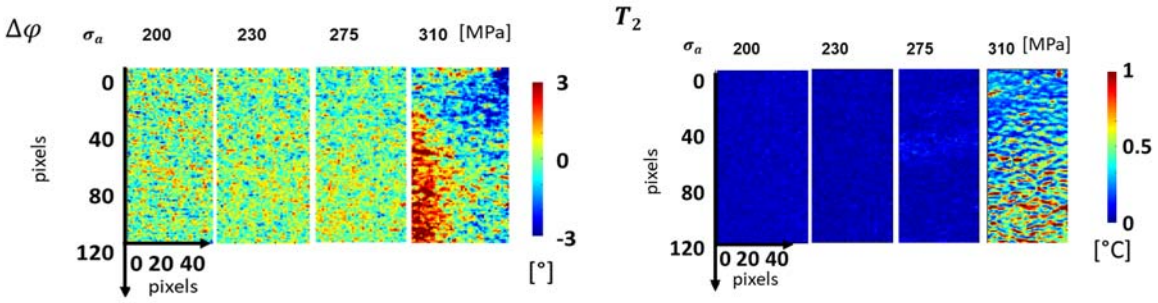

(c) (d)

Figure 6. Maps resulting from the analysis of energy-based methods related to thermal parameters at R=-1, sample P2.

4.2. Quantitative analysis of the data

The quantitative analysis of the parameters extracted from thermal signal and mechanical signal is discussed in the present section by comparing the results in terms of $\Delta T_{0_{95prc}}$, $T_{1_{95prc}}/\Delta\sigma$, $\Delta\varphi$, $T_{2_{95prc}}$ and ΔW curves at two stress ratios, figure 7.

By observing the all the curves of figure 7 one can observe that all the parameters are related to stress amplitude by a non-linear relationship. Moreover, the values of the parameter at R=-1, are in general higher than those at R=0.1, due to the higher dissipations occurring in fully reversed loading condition especially for those loading levels near the failure.

The mean temperature variations $\Delta T_{0_{95prc}}$, figure 7a, present for both the data series at two stress ratios typical nonlinear behaviour where the extreme data points of the series at R=-1 present temperature values near 120 °C.

In figure 7b, the thermoelastic signal, $T_{1_{95prc}}/\Delta\sigma$, of the series at R=0.1 presents a smooth nonlinear behaviour while the series at R=-1 presents a more marked signal increase in correspondence to the stress amplitude of 310 MPa.

The thermoelastic phase shift $\Delta\varphi$, figure 7c, is characterised by the same nonlinear behaviour at two stress ration, and an initial under no damage conditions small phase changes for both the stress ratios and a more pronounced phase variation at respectively stress level of 200 MPa for the data series at R=0.1 and 300 MPa for the data series at R=-1. The last points of this latter data series have been excluded as they compromised the scale values by flattening the curves at R=0.1.

The same consideration can be made for the data series $T_{2_{95prc}}$ and ΔW figure 7d-e, where the signal variations are less pronounced at the stress ratio of 0.1 if compared to the variations at R=-1. In this case the higher values of the parameter $T_{2_{95prc}}$ and ΔW at R=-1 flatten the scale value making difficult to detect the signal variations at R=0.1. This demonstrate the great analogy between these two parameters representing an estimations of energy dissipated in heating and mechanical strain energy supplied.

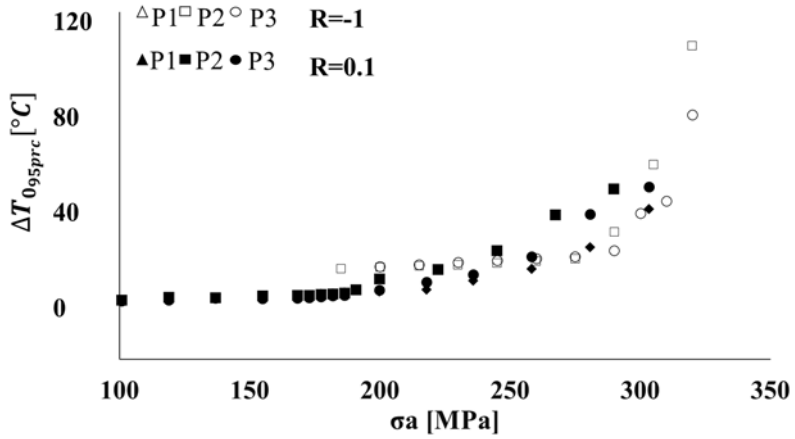
△P1□P2○P3 R=-1
▲P1■P2●P3 R=0.1
ΔT_{095prc} [°C]
120
80
40
0
100
150
200
250
300
350
σa [MPa]

(a)

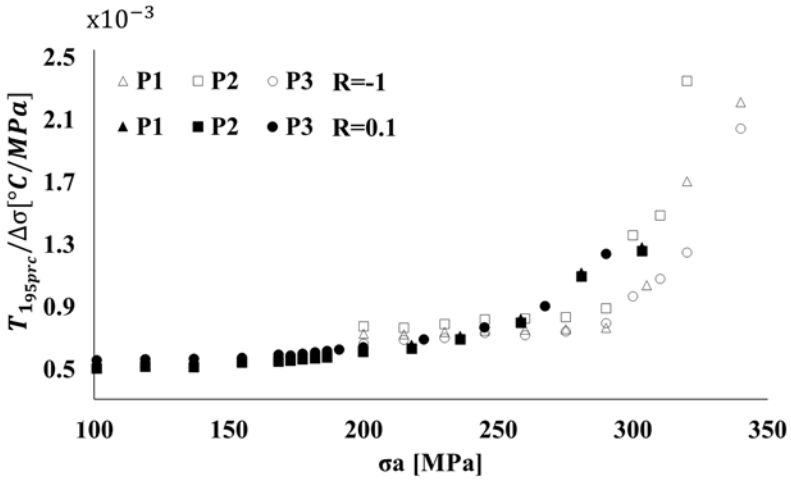
x10⁻³
△P1 □P2 ○P3 R=-1
▲P1 ■P2 ●P3 R=0.1
$T_{195prc}/\Delta\sigma$[°C/MPa]
2.5
2.1
1.7
1.3
0.9
0.5
100
150
200
250
300
350
σa [MPa]

(b)

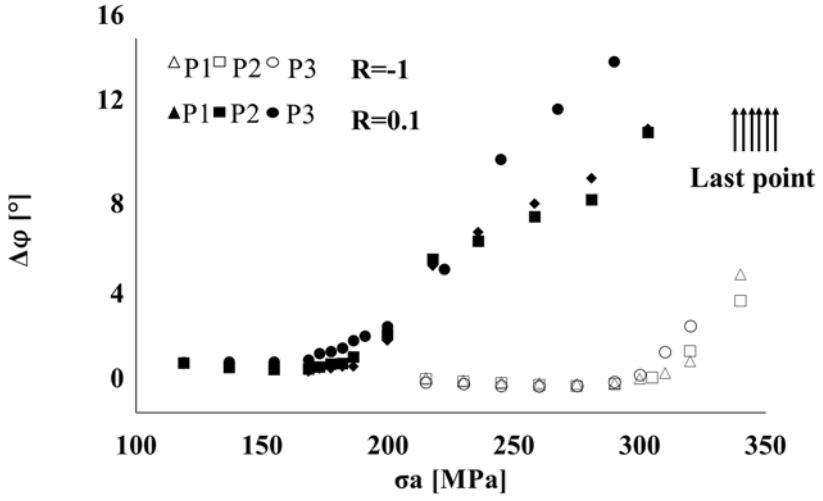
△P1□P2○P3 R=-1
▲P1■P2●P3 R=0.1
Last point
Δφ [°]
16
12
8
4
0
100
150
200
250
300
350
σa [MPa]

(c)

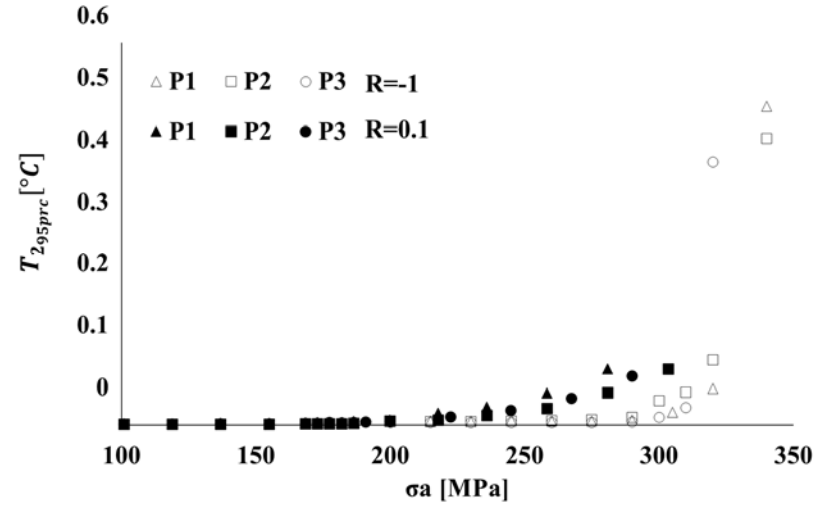

(d)

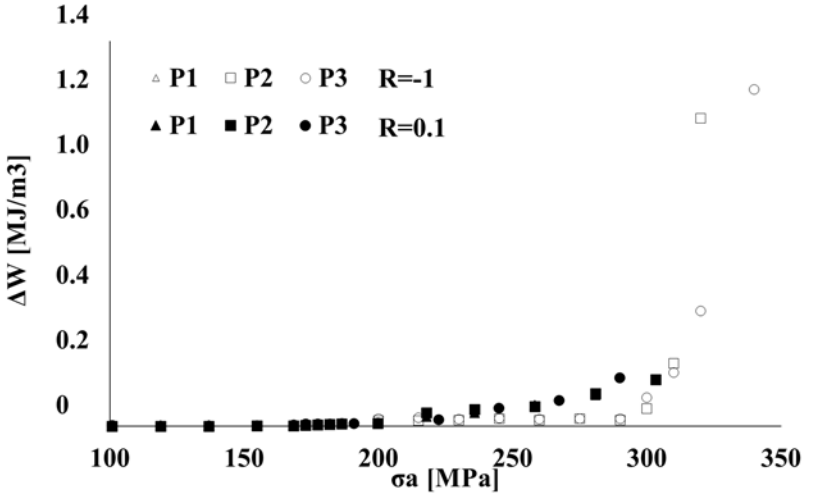

(e)

Figure 7. Curves obtained by using energy-based methods: (a) $\Delta T_{0_{95prc}}$, (b) $T_{1_{95prc}}/\Delta\sigma$, (c) $\Delta\varphi$, (d) $T_{2_{95prc}}$, (e) ΔW.

In the present section, it is also possible to compare the trend of the parameter $T_{2_{95prc}}$ and the one of ΔW. As found by several authors [7-10,23], the temperature variations occurring at twice the mechanical frequency are related to the intrinsic dissipation that can be evaluated by estimating the area under the hysteresis loop [10].

By observing figure 7d and 7e the $T_{2_{95prc}}$ and ΔW at both stress ratios the strict correlation in the trend of these two parameters is evident. For the case of stress ratio R=0.1 even if the behaviour of the two parameter is continuously increasing, the two nonlinear curves exhibit a preliminary part characterised by lower signal variations and a significant signal increase at a stress level of about 200 MPa. For the curves of the samples tested at R=-1, the behaviour of $T_{2_{95prc}}$ and ΔW present an initial trend characterised by lower signal variations and an unambiguous signals increase at stress amplitude of 300 MPa.

This result demonstrates for the specific material in these specific conditions the possibility to further estimate the area under the hysteresis loop by simply measuring the second harmonic component of the temperature, clearly by means of a suitable calibration.

4.3. The influence of the temperature variations T_0 on thermoelastic signal variations

In the present section another consideration can be made about the influence of the temperature T_0 on thermoelastic signal variations. In figure 8 are reported the curves for the tests performed at the two stress ratio of the thermoelastic signal referred to both the mean temperature and the stress amplitude, $T_{1_{95prc}}/\ T_0\,\Delta\sigma$.

In figure 8a the signal for the stress ratio of 0.1 presents an initial low signal variation behaviour common for all the tested samples and a second trend characterised by higher data dispersion for the series $T_{1_{95prc}}/\ T_0\,\Delta\sigma$. In this case, the thermoelastic signal seems to be insensitive to the joint effect of the temperature and stress increase. One can only conclude that the effect of T_0 does not affect the signal behaviour but just add some noise. So that, the study of the damage is not compromised. In figure 8b, for the stress ratio R=-1, the influence of T_0 (mostly for sample 1 and 3) makes the $T_{1_{95prc}}$ series noisier. This can explain the initial decrease of the curves of sample 1 and 3 in figure 8b. However, also in this case the $T_{1_{95prc}}/T_0\,\Delta\sigma$ increase occurs at a stress level of 300 MPa, so that it is possible to study the damage behaviour by evaluation $T_{1_{95prc}}/\ T_0\,\Delta\sigma$ or $T_{1_{95prc}}/\ \Delta\sigma$ parameters.

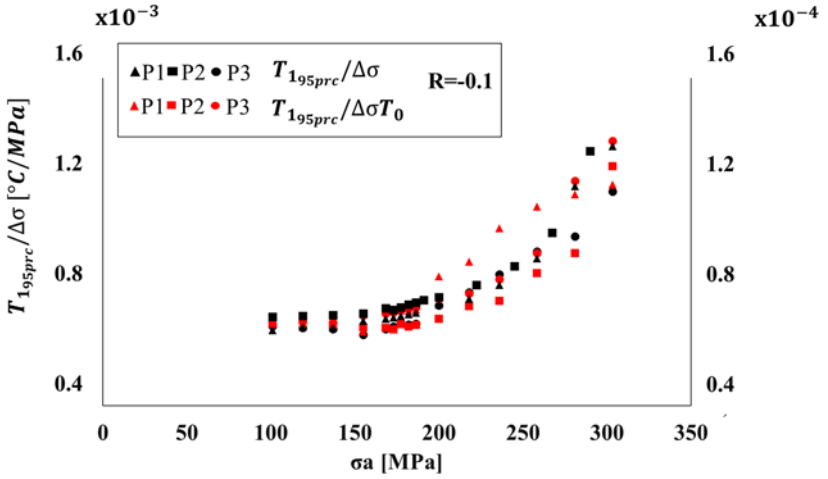

(a)

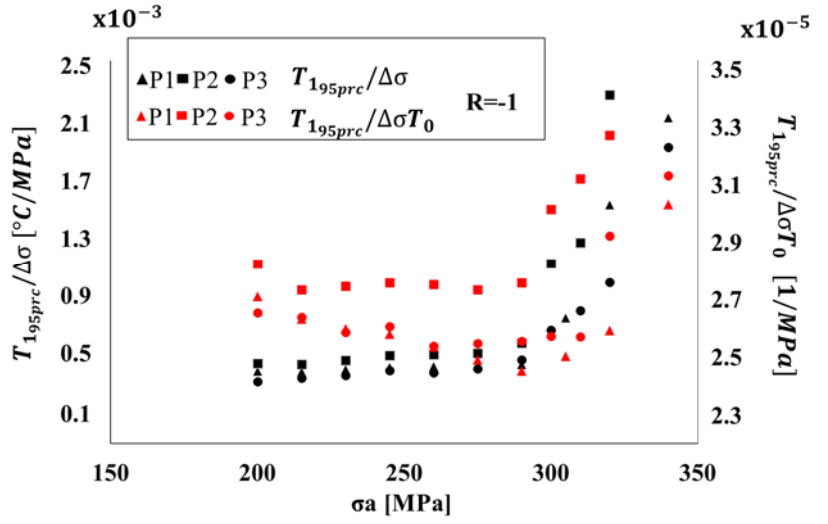

(b)

Figure 8. Effect of the temperature variations T_0 on thermoelastic signal at (a) R=0.1 (b) R=-1.

Conclusions

In the present work, the mechanical characterization of C45 steel has been performed. Six samples have been tested by using an accelerated stepwise loading procedure: three samples for the tests at R=0.1 and three for those at R=-1. The equipment was composed by an infrared camera that allowed thermal parameter assessment and an extensometer that measured strains and loads to evaluate the area under the hysteresis loop.

The assessment of thermal ($\Delta T_{0_{95prc}}$, $T_{1_{95prc}}/\Delta\sigma$, $\Delta\varphi$,$T_{2_{95prc}}$) and mechanical (ΔW) parameters allowed to study quantitatively and qualitatively the energy under different point of views and to study the material damage. In particular, by examining the trends it is possible to conclude:

- there is a great agreement for a specific imposed stress ratio between thermal and mechanical parameters referring to the material damage;
- by assessing the different parameters it is possible to assess an overview of damage processes ongoing in the material;
- thermal parameter $T_{2_{95prc}}$ is just an estimation of the energy dissipated as heat and then of the total energy provided to the material, but its trend is similar to ΔW, and it can be used to indirectly assess the area under the hysteresis loop in all the cases where it is difficult;
- the effect of the temperature T_0 on the thermoelastic signal variation does not compromise the material damage behaviour assessment, but just $T_{1_{95prc}}/\ T_0\ \Delta\sigma$ is noisier than $T_{1_{95prc}}/\ \Delta\sigma$ especially when temperature increase is higher.

References

[1] R. De Finis, D. Palumbo , F. Ancona., U. Galietti 2015 *Int. J. Fatigue* **96** 74-88.
[2] MP. Luong 1995 *Nucl. Eng. Des.* **158** 363-373.
[3] Meneghetti G 2007 *Int. J. Fatigue* **29** 81-94.
[4] Polák J, Petrenec M, Kruml T, Chlupová A 2011 *Proc Eng* 2011 vol10 p.568–577.
[5] Risitano A, Risitano G. 2009 *Frattura ed Integrità Strutturale* **9** 113-124.
[6] Krapez JK, Pacou D, Gardette G 2000 *Quantitative Infrared Thermography* **6** 277-82.
[7] Enke NF 1989 *Proc. SPIE 1084, Stress and Vibration: Recent Developments in Industrial Measurement and Analysis* doi: 10.1117/12.952908
[8] Enke NF, Sandor BI 1988 *Proc. Of the VI Int. Congress on Experimental Mechanics* p.830-5.
[9] De Finis R, Palumbo D, Galietti U 2016 *Journal of Imaging* **2** 32.
[10] De Finis R, Palumbo D 2020 *Materials* **13** 1-18.
[11] La Rosa G, Risitano A 2013 *Int. J. Fatigue* **22** 65-73.
[12] Curà F, Curti G, Sesana R 2005 *Int. J. Fatigue* **27** 453-59.
[13] Uhmenofer T , Medgenberg J 2009 *Int. J. Fatigue* **31** 130-7.
[14] Risitano A, Risitano G 2010 *Workshop International Group of Fracture (Forni di Sopra*).
[15] Morabito AE, Chrysocos C, Dattoma V, Galietti U 2007 *Int. J. Fatigue* **29** 977-84.
[16] Boulanger T, Chrysochoos A , Mabru C , Galtier C 2006 *Int. J. Fatigue* **26** 221-229.
[17] Sakagami T, Kubo S, Tamura E, Nishimura T 2015 *International Conference of Fracture ICF11 (Catania, Italy).*
[18] Chrysochoos A, Huon V, Jourdsan F, Muracciole JM, Peyroux R , Wattrisse, B 2009 *Strain* **46** 117-130.
[19] Pittaresi G, Patterson EA 2003 *J. Strain Anal. Eng. Des.* **38** 405-17.
[20] Harwood N, Cummings W 1991 *Thermoelastic Stress Analysis* (New York: National Engineering Laboratory, Adam Hilger).
[21] Diaz FA, Patterson EA, Tomlinson RA, Tomlison JR, Yates JR 2004 *Fatigue Fract. Eng. Mat. Struct.* **27** 571-83.
[22] Wang WJ, Dulieu-barton JM, Li Q 2010 *Exp. Mech.* **50** 449-61.
[23] De Finis R, Palumbo D, Galietti U 2018 *Fatigue Fract. Eng. Mat. Struct.* **42** 267-83.
[24] Morrow JD 1964 ASTM Spec. Tech. Publ. **378** 45.

[25] Ellyin F, Kujawski D 1984 *J. Pressure Vessel Technol*. **106** 34.
[26] Kliman V, Bily M 1984 *Materials Science and Engineering* **68** 11-18.
[27] ASTM E 466-96 *Standard Practice for Conducting Force Controlled Constant Amplitude Axial Fatigue Tests of Metallic Materials*.
[28] Diagnostic Engineering Solutions (DES srl) 2015 *IRTA Manual* (Des srl: Bari, Italy).